Naseer *et al. Cell Communication and Signaling* (2025) 23:221
https://doi.org/10.1186/s12964-025-02212-0

Cell Communication and Signaling

RESEARCH Open Access

Differential regulation of mTORC2 signalling by type I and type II calreticulin (CALR) driver mutations of myeloproliferative neoplasm

Saadia Naseer[1], Aditi Singh[1], Saurabh Shrivastva[1], Rishi Kant Singh[1], Shayeri Chowdhury[1], Chinmoy Sankar Dey[1] and Anita Roy[1*]

Abstract

Calreticulin (CALR) is an endoplasmic reticulum chaperone. Frameshift mutations in CALR were discovered in patients with myeloproliferative neoplasm showing increased platelet counts. The frameshift was observed in the last exon of CALR, leading to a novel C-terminal tail. Calreticulin mutations were categorised into Type I and Type II depending upon the extent of retention of CALR WT sequences. Clinically, Type I mutations induced myelofibrosis, while Type II mutations were associated with early onset of the disease. Both mutations induced ligand-independent activation of the thrombopoietin receptor (TpoR) and consequently enhanced platelet production. However, no specific difference in signalling mechanism could be demonstrated between them. Using over-expression of CALR WT, CALR Δ52 (Type I) and CALR ins5 (Type II) in HEK cells, we showed that Type I CALR mutations downregulated the basal mTORC2 signalling without affecting mTORC1. The decrease in basal mTORC2 signalling was attributed to CALR Δ52-induced increased expression of c-JUN through occupation of the enhancer sequences of *jun*. Furthermore, increased c-JUN expression decreased the expression of RICTOR, a component of mTORC2. Strikingly, overexpression of RICTOR or knockdown of c-JUN reversed the inhibitory effect of CALR Δ52 on mTORC2 activity. Finally, we demonstrated that CALR Δ52 decreased the glucose uptake and cellular ATP levels in a c-JUN-mTORC2-dependent manner. These findings not only contribute to our understanding of the molecular mechanisms underlying mutant CALR driven myeloproliferative neoplasm but also provide potential therapeutic targets against the disease.

*Correspondence:
Anita Roy
anita.roy@bioschool.iitd.ac.in

Full list of author information is available at the end of the article

Graphical abstract

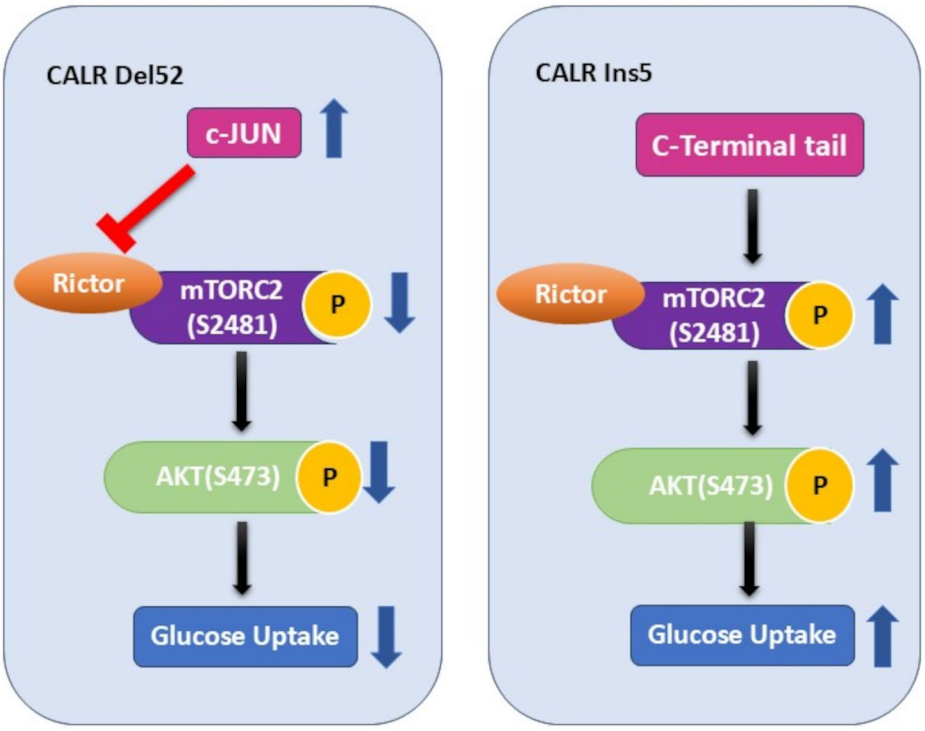

Keywords CALR, Signalling, mTORC2, c-JUN, ChIP, Glucose uptake

Introduction

Calreticulin (CALR) is an endoplasmic reticulum (ER) chaperone that works in concert with calnexin and Erp57 to fold nascent polypeptides [1, 2]. The +1 frameshift mutations in CALR have been detected in patients with myeloproliferative neoplasms (MPN) displaying megakaryocyte hyperplasia and increased platelet counts [3, 4]. All mutations occurred in the last exon (exon 9) of *calr*, leading to a complete (Type I) or partial (Type II) loss of the negatively charged tail. The frameshift mutation also resulted in the loss of the terminal ER-retrieval sequence (KDEL) [3, 4]. Mechanistically, the CALR mutations were found to activate the thrombopoietin receptor (TpoR) in a ligand-independent manner, leading to the activation of JAK2-STAT1/3/5 signalling and cytokine-independent proliferation. Both Type I and Type II CALR mutations were equally effective in carrying out ligand-independent activation of TpoR [5, 6]. However, significant differences in patient outcomes have been observed between Type I and Type II CALR mutations. Type I mutations were associated more with myelofibrosis, while Type II mutations had a younger age at presentation and, in general, a more aggressive disease phenotype [7]. The presence of the mutant CALRs with a novel C-terminal tail in the different sub-cellular compartments may induce novel signalling pathways that were not affected by the ER restricted CALR WT. This was evident through the recent studies which used mammalian target of rapamycin (mTOR) inhibitors such as rapamycin, everolimus and mTOR/PI3K inhibitor BEZ235 and found a reduction in mutant CALR-dependent myeloproliferation [8, 9]. Since mutant CALRs drove TpoR/JAK2 dependent activation of PI3K/Akt, it was difficult to interpret in these experiments if mutant CALRs independently induced Akt-mTOR signalling.

Using overexpression of CALR WT, CALR Δ52 (Type I) and CALR ins5 (Type II), we investigated whether mutant CALRs could activate mTOR signalling independent of TpoR. This is important since CALR mutation arising in the hematopoietic stem cells penetrates both the myeloid and lymphoid compartments and is thus present in cells devoid of TpoR [10]. Our results showed that the Type I (CALR Δ52) and Type II (CALR ins5) mutants differed with respect to their effects on mTOR complex 2 (mTORC2) without affecting the mTOR complex 1 (mTORC1). This was attributed to the increased occupation of enhancer regions of *jun* by CALR Δ52, leading to the enhanced expression of c-JUN. c-JUN destabilised the mTORC2 by reducing the expression of RICTOR. For the first time, our study identifies a

crucial difference between Type I and Type II mutations of CALR in terms of basal mTORC2 signalling.

Results

Type I and Type II CALR mutations differentially regulate basal mTORC2 activity

We investigated whether CALR Type I, and Type II mutations affect basal mTORC1 and mTORC2 signalling. We overexpressed HA-tagged CALR WT, Δ52, and ins5 in HEK293 cells and checked the basal activation of mTORC1 and mTORC2 complexes. mTOR complex 1 can be activated by Akt phosphorylated at T308. This leads to the phosphorylation of the downstream effectors, S6K and 4EBP1 [11]. On the other hand, activated mTOR complex 2 phosphorylates Akt S473 and NDRG1 T346 (Fig. 1A). We observed a decrease in the phosphorylation of TOR complex 2 specific mTOR S2481 and its downstream effectors Akt S473 and NDRG1 T346 in cells expressing CALR Δ52 compared to CALR WT in HEK and U2OS cell lines (Fig. 1B and S1A-B). On the other hand, CALR ins5 exhibited increased phosphorylation of mTOR S2481 along with the downstream Akt S473, and

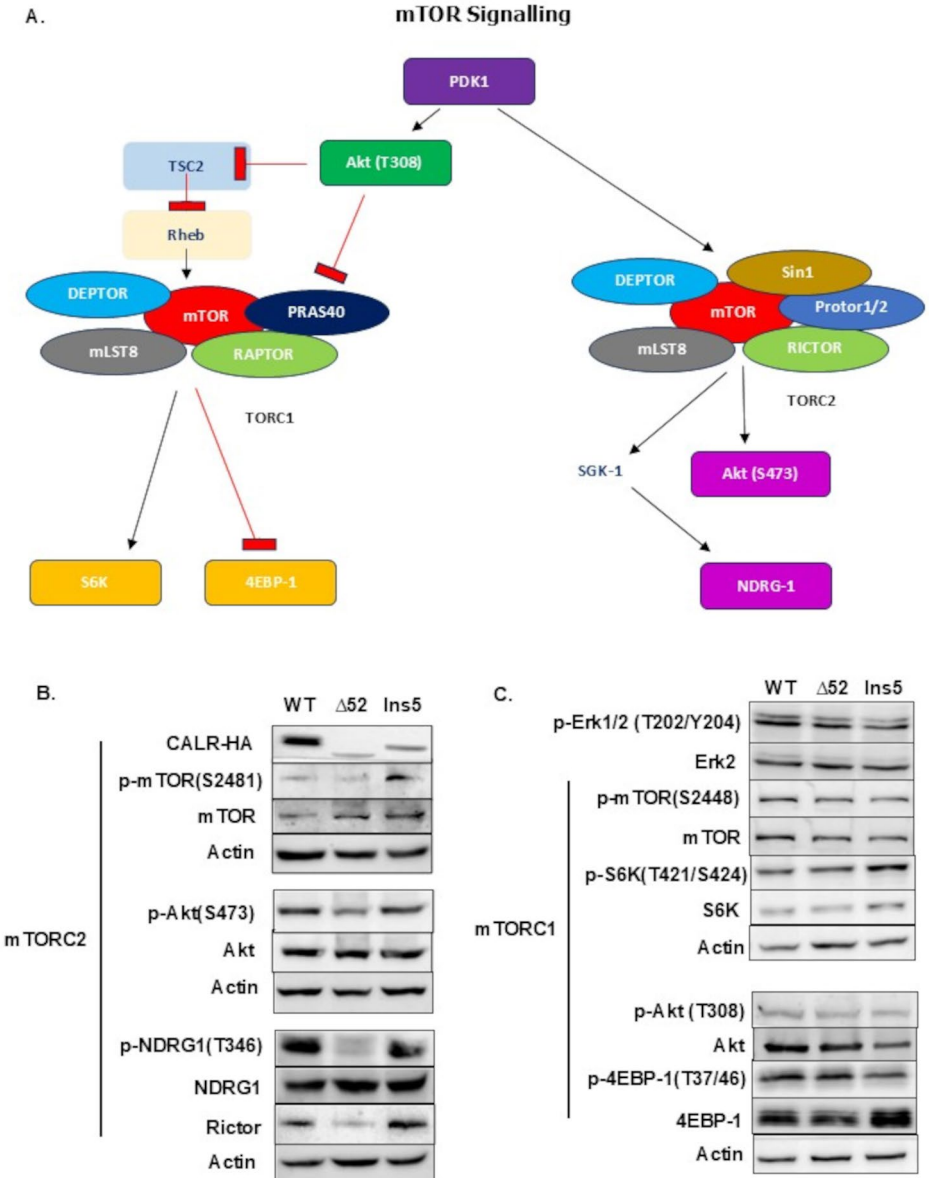

Fig. 1 CALR mutants differentially regulate mTORC2 signalling. **(A)** Schematic diagram to delineate mTOR signalling and its downstream targets. **(B-C)** Representative western blots for HEK293 cells overexpressing CALR-WT, CALR-Δ52, and CALR ins5 (HA-tagged CALR constructs) harvested 24 h post-transfection for immunoblotting (**B**) mTORC2 specific targets (mTOR-S2481, mTOR, Akt-S473, Akt, NDRG-1 T346, NDRG-1) and Rictor. Actin was used as the loading control. ($n=3$ biological replicates) **(C)** mTORC1 specific targets (mTOR-S2448, mTOR, S6K -T421/S424, S6K, 4EBP-1 T37/46, 4EBP-1), Akt T308, Akt, Erk-T202/Y204 and Erk2. Actin was used as the loading control. ($n=3$ biological replicates)

NDRG1 T346 (Fig. 1B). However, the phosphorylation of mTORC1 S2448 and Akt T308 did not change for either of the CALR mutants (Fig. 1C). This showed that both Type I and Type II CALR mutations differentially regulated mTORC2 activity. Importantly, no eminent differences between the endogenous CALR and overexpressed CALR WT was observed in terms of basal mTORC1 and mTORC2 activity (Figure S2A-B).

CALR WT Truncation mutants activate basal mTOR activity

Since the Type I and II mutations differed in the extent to which they retained the CALR WT tail sequence, we investigated whether progressive deletion of the CALR WT tail could recapitulate the basal mTORC2 signalling observed in the presence of CALR Δ52 and ins5. We generated wildtype truncation tail mutants (CALR WT Δ15, Δ30, Δ45 and ΔExon9) to study the dependence of CALR WT C-terminal tail on the activity of the mTOR complex (Fig. 2A). Of note, the CALR WT Δ45 and Δ30 truncation mutations resembled CALR Δ52 and ins5, respectively, in terms of the length of the CALR WT sequences retained (Fig. 2A). Moreover, all truncation mutants were secreted and thus, detected on the cell surface (Figure S3A-B). We, therefore, expected that these would mimic the CALR Type I and Type II phenotypes. Surprisingly, progressive truncation of CALR WT tail resulted in an increase in the phosphorylation of both mTOR S2481 and mTOR S2448 (Fig. 2B-C). A corresponding increase in the phosphorylation of Akt S473 was observed without any change in the phosphorylation of Akt T308 (Fig. 2B-C). Contrary to CALR Δ52, CALR WT Δ45 cells exhibited increased mTORC2 activity as seen from

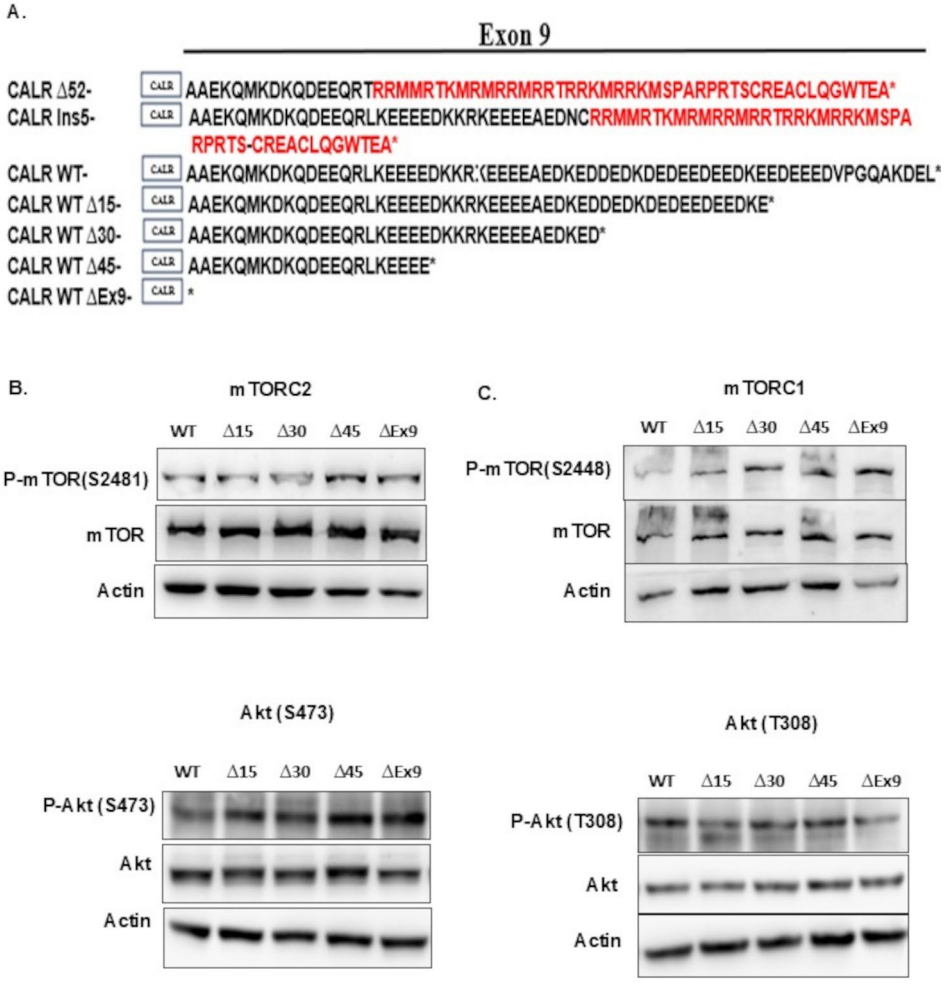

Fig. 2 CALR WT truncation mutants activate basal mTOR activity **(A)** Comparative sequence of CALR WT and its truncated tail mutants (CALR Δ15, Δ30, Δ45 and ΔEx9) with CALR Δ52 (Type I) and CALR ins5 (Type II) mutants. The sequence highlighted in red represents the common mutant tail in both Type I and Type II CALR mutants. (**B**, **C**). Representative western blots for transfected CALR WT and its truncation tail mutants (CALR Δ15, Δ30, Δ45 and ΔEx9) in HEK 293 cells harvested 24 h post-transfection for examining (**B**) mTORC2 (S2481) and Akt S473 phosphorylation relative to total proteins mTOR and Akt respectively. Actin level indicates loading control. ($n = 3$ biological replicates). **(C)** mTORC1 (S2448) and Akt T308 phosphorylation relative to total proteins mTOR and Akt, respectively. Actin level indicates loading control. ($n = 3$ biological replicates)

the increased phosphorylation of mTOR S2481 and its downstream target Akt S473 (Fig. 2B). Thus, the effects of CALR Δ52 on mTORC2 extended beyond a loss of function characteristic caused by the loss of CALR WT C-terminus. As expected, CALR WT Δ30 like CALR ins5 showed an increase in basal mTORC2 signalling (Fig. 2B). Together, the data indicated that the mTORC2 complex could be activated by truncation of CALR WT tail. However, CALR Δ52 showed anomalous down-modulation of mTORC2 activity creating a crucial difference between CALR Type I and Type II mutations.

c-JUN downregulates mTORC2 activity in CALR Type I mutation through RICTOR

c-JUN, an AP-1 family member transcription factor encoded by *jun* is a downstream target of JNK mediated phosphorylation. JNK mediated mTORC2 regulation was shown previously [12]. We observed elevated c-JUN expression (Fig. 3A and S4A), which correlated with diminished RICTOR expression in CALR Δ52 expressing cells (Fig. 1B). The down-modulation of mTORC2 activity and its target, Akt S473 by CALR Δ52, decreased the phosphorylation of FOXO1 at S256 (a direct downstream target for Akt S473) (Fig. 3B). Interestingly, we also observed an increase in the transcription of FOXO1 with CALR Δ52 (Figure S4B). Overexpression of c-JUN, resulted in reduced expression of RICTOR along with phosphorylation of mTORC2 (S2481) and Akt S473, mirroring the CALR Δ52 phenotype (Fig. 3C). Finally, siRNA-mediated silencing of c-JUN in CALR Δ52 expressing cells reversed the expression of mTORC2 phosphorylation and its downstream target Akt S473 (Fig. 3D). This established c-JUN mediated downmodulation of the mTORC2 activity in CALR Type I mutant expressing cells.

To rescue the downregulation of basal mTORC2 signalling in the presence of CALR Δ52, we overexpressed mTORC2 components RICTOR and mSIN1 in a Type I CALR background. We observed an increase in mTORC2 phosphorylation without any change in the phosphorylation of Akt S473 with either RICTOR or mSIN1 overexpression (Fig. 3E). However, a combination of RICTOR and mSIN1 rescued the mTORC2 activity, including increased expression of phospho-Akt S473. This indicated a compromised mTOR complex 2 assembly in Type I CALR mutant expressing cells.

CALR Δ52 occupies the distal enhancer of *jun*

Mutant CALRs have been shown to be present in the nucleus [13]. Previous report had linked nuclear CALR Δ52 with increased chromatin occupancy of Fli1 at the TpoR promoter leading to enhanced megakaryopoiesis and platelet production [14]. We therefore asked if CALR WT, Δ52 or ins5 could influence *jun* expression through chromatin modulation by binding to its promoter and/or enhancer regions (Fig. 4A).

Chromatin immunoprecipitation of CALR WT/Δ52/ins5 revealed a significant enrichment of CALR Δ52 at the distal enhancer regions 2 and 3 of *jun* (Fig. 4B). No significant enrichment was observed with CALR WT or ins5. This agreed with our previous observation of increased c-JUN expression and activity in CALR Δ52 expressing cells (Fig. 3). Thus, CALR Δ52 enhanced the expression of c-JUN through direct binding at the distal enhancer of *jun*.

Type I and Type II CALR mutations render basal Akt activation sensitive to inhibition by MK2206, GDC0068 and PDK1 inhibition

Since, basal phosphorylation of Akt at Ser473 was found to differ between CALR Δ52 and ins5, we asked whether the various Akt inhibitors behaved differentially in the presence of the CALR WT and the two CALR mutants. We used MK2206 (an allosteric Akt inhibitor), GDC0068 (competitive Akt inhibitor) and GSK2334470 (PDK1 inhibitor) [15]. Our results showed that all three inhibitors abolished the activity of both mTOR complexes (C1 and C2) irrespective of whether the cells expressed CALR WT, CALR Δ52 or ins5 mutation (Figure S5A-B). Of note, GDC0068, an ATP competitive inhibitor is known to increase the phosphorylation of AKT at S473 and T308 without further causing an increase in the downstream signalling through mTOR and S6K [16, 17]. We observed a similar pattern of GDC0068 induced inhibition of mTOR signalling despite a paradoxical increase in AKT S473 and T308 phosphorylation (Figure S5A-B). This indicated that despite the differences in basal TOR complex 1 and 2 activity, both Type I and Type II CALR mutations were sensitive to PDK1 and Akt inhibitors.

c-JUN downregulated glucose uptake in Type I CALR mutation

Complex 2 of mTOR is a regulator of glucose metabolism and cellular response to various nutrients [18]. Therefore, to understand the cellular energetics in the presence of CALR mutants, we analysed glucose uptake using the fluorescent glucose analogue 2-NBDG. We observed a significantly lower glucose uptake in CALR Δ52 as compared to the CALR WT (Fig. 5A). This correlated with the CALR Type I mediated downregulation of the kinase activity of mTORC2 (Fig. 1B). Additionally, we observed an increase in total cellular ATP levels in CALR ins5 cells as compared to CALR WT and CALR Δ52 (Fig. 5B). Furthermore, we supplemented CALR Δ52 cells with RICTOR and mSIN1 to enhance mTORC2 activity. Our results showed that the overexpression of either RICTOR or mSIN1 or a combination of both increased the glucose uptake in cells expressing CALR Δ52 (Fig. 5C). Strikingly,

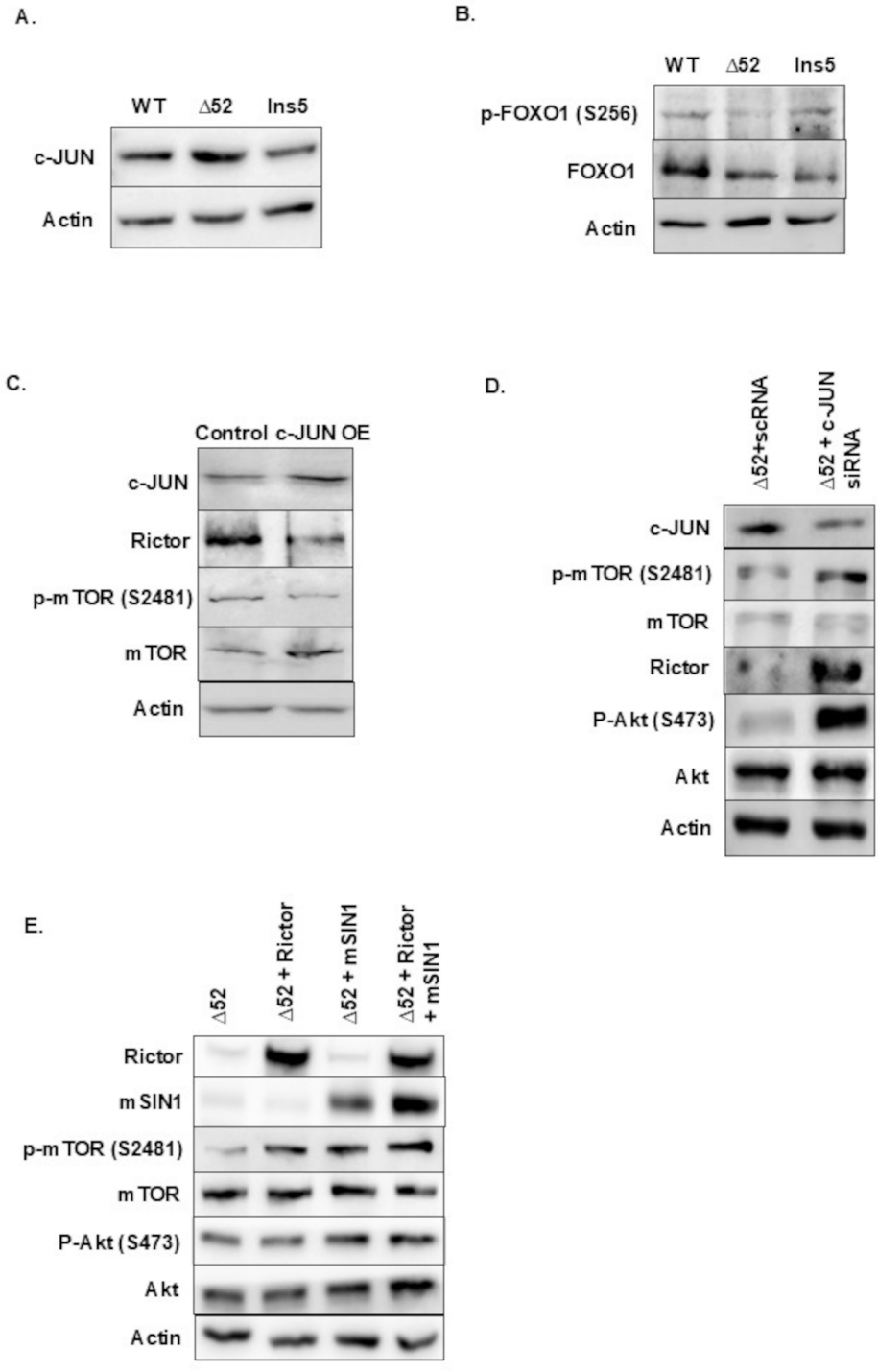

Fig. 3 c-JUN is upregulated specifically in CALR Type I mutant to downmodulate mTORC2 mediated signalling. **(A**, **B)** HEK 293 cells were transfected with CALR constructs, CALR WT, Δ52 and ins5 and harvested 24 h after transfection for immunoblotting. **(A)** Expression of c-JUN **(B)** Expression of p-FOXO1 (S256) relative to FOXO1 level. Actin is the loading control. ($n=3$ biological replicates). **(C)** Representative western blot for HEK 293 control and overexpressing c-JUN (c-JUN OE). The cells were lysed and probed with Rictor, mTORC2 (S2481) relative to mTOR. Actin is the loading control. ($n=3$ biological replicates). **(D)** Representative western blot for HEK293 cells transfected with CALR Δ52 along with either scrambled siRNA (Δ52 + scRNA) or c-JUN siRNA to examine the mTORC2 specific phosphorylation (mTORC2 (S2481) and its downstream effector Akt S473) relative to total proteins mTOR and Akt respectively) along with Rictor. Actin is the loading control. ($n=3$ biological replicates). **(E)** Representative western blot for overexpressing CALR Δ52 co-transfected with either RICTOR or mSIN1 or both in HEK293. CALR Δ52 expressing cells are control sample. The blots were probed for mTORC2 specific targets (mTORC2 S2481) and Akt S473 phosphorylation relative to total proteins mTOR and Akt respectively). Actin is the loading control. ($n=3$ biological replicates)

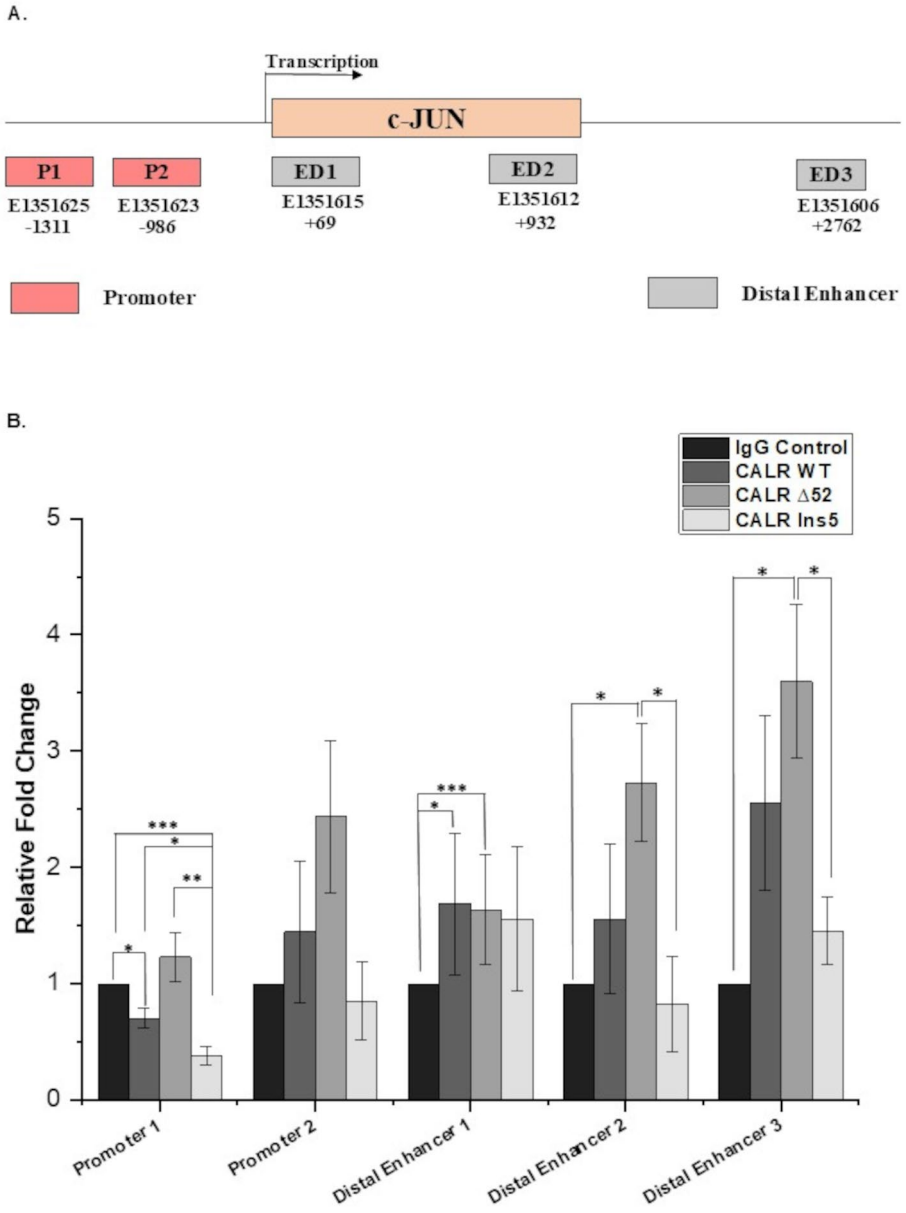

Fig. 4 CALR Type I mutant occupies the distal enhancer regions in c-JUN. **(A)** Schematic diagram representing promoter and distal enhancer regions along with their accession number and site used in the ChIP analysis. **(B)** ChIP-qPCR analysis of CALR WT/Δ52/ins5 transfected samples in HEK 293 cells for *jun* promoter and distal enhancer regions. Fold change is relative to the IgG control. Data is represented as the mean ± SEM. ANOVA was performed to calculate the statistical significance. Asterisk (*) indicates statistical significance between test conditions and IgG control while significance between test conditions is indicated separately. *$p < 0.05$, **$p < 0.01$, ***$p < 0.001$

co-expression of RICTOR and mSIN1 significantly increased the cellular ATP levels as compared to CALR Δ52 control cells (Fig. 5D). Together the data indicates CALR Δ52 destabilised mTOR complex 2 assembly. Our earlier data showed an increased mTORC2 activity upon knockdown of c-JUN (Fig. 3D). Consequently, we studied glucose uptake in CALR Δ52 after knockdown of c-JUN and observed a significant enhancement in the glucose uptake in these cells compared to CALR Δ52 expressing cells (Fig. 5E). Taken together, our results showed that whereas Type II CALR mutations (CALR ins5) increased mTORC2 activity and glucose uptake, Type I mutations (CALR Δ52) produced low basal mTORC2 activity and, consequently, low glucose uptake and ATP levels.

c-JUN- mTORC2-AKT axis is conserved across MPN cell line models

Ba/F3 and K562 cell lines expressing CALR mutations have been extensively used to gain mechanistic insights into pathogenesis of myeloproliferative neoplasms

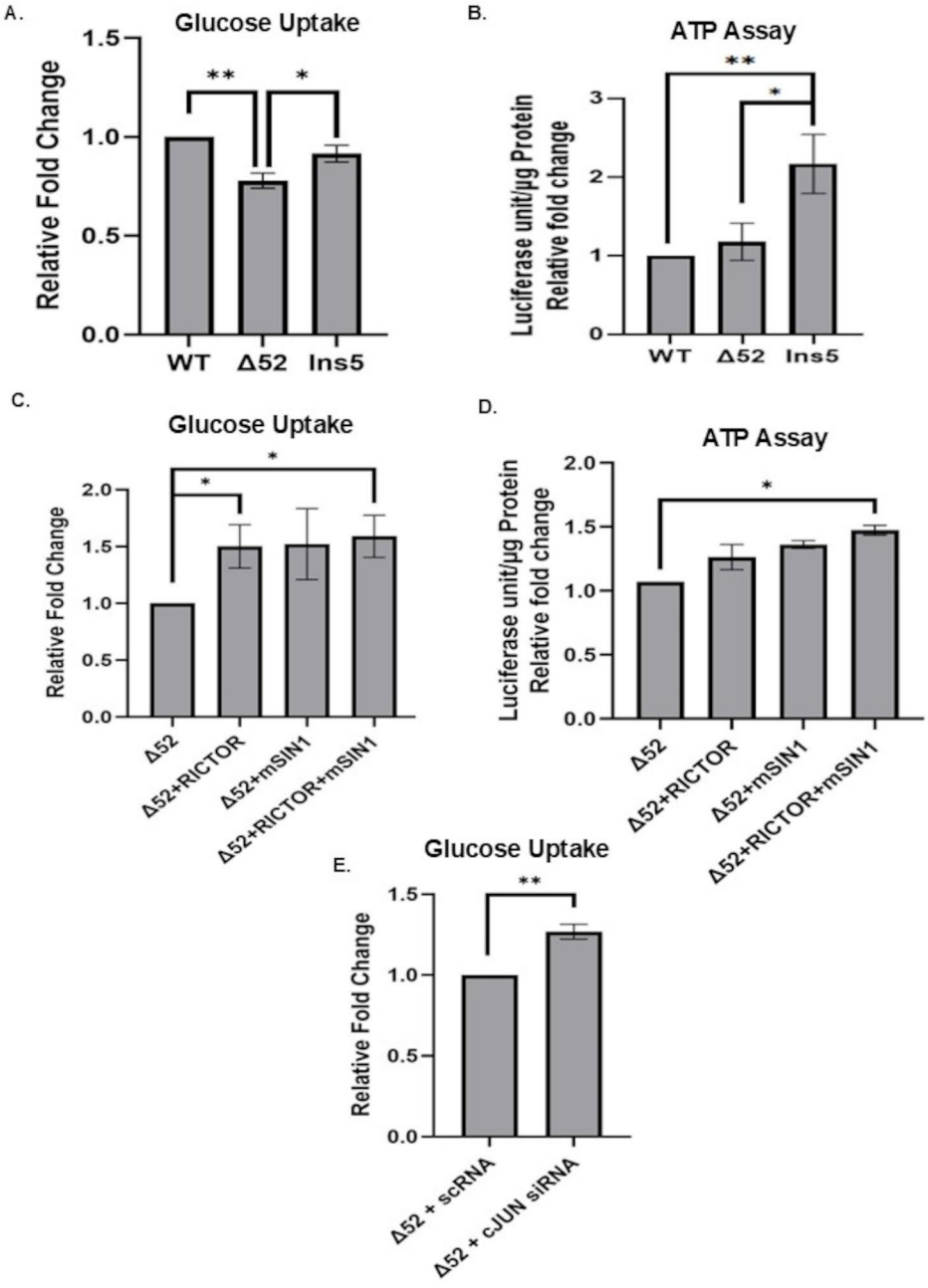

Fig. 5 CALR mutants modulate glucose uptake. **(A)** Glucose uptake in CALR WT, CALR Δ52, and CALR ins5 (mCherry tagged) expressing HEK293 cells were analysed by flow cytometry using 2-NBDG. CALR WT and mutants expressing cells were starved for an hour, followed by 30 min of treatment with 2-NBDG in the dark condition. Data is represented as the relative fold change with respect to CALR WT overexpressing cells. ($n = 7$). The statistical significance was measured through ANOVA followed by Tukey's post hoc test. **(B)** ATP determination assay for HEK 293 cells expressing CALR WT, CALR Δ52, and CALR ins5. Data is represented as the relative fold change with respect to CALR WT overexpressing cells. ($n = 6$). The statistical significance was measured through ANOVA followed by Tukey's post hoc test. **(C)** Glucose uptake in CALR Δ52 expressing cells with either RICTOR or mSIN1 or both in HEK293 cells analysed by flow cytometry using 2-NBDG. Data is represented as the relative fold change with respect to CALR Δ52 overexpressing cells. ($n = 3$). The student's t-test was used to calculate the statistical significance. **(D)** ATP determination assay for HEK cells expressing CALR Δ52 along with either RICTOR or mSIN1 or both. Data is represented as the relative fold change with respect to CALR Δ52 overexpressing cells. ($n = 3$). The student's t-test was used to calculate the statistical significance. **(E)** Glucose uptake in CALR Δ52 expressing cells with scrambled siRNA (Δ52 + scRNA) or with siRNA against c-JUN in HEK293 cells analysed by flow cytometry. Data is represented as the relative fold change with respect to CALR Δ52 overexpressing cells. ($n = 3$). Data is represented as mean ± SEM. Asterisk (*) indicates statistical significance measured through student's t-test. *$p < 0.05$ and **$p < 0.01$

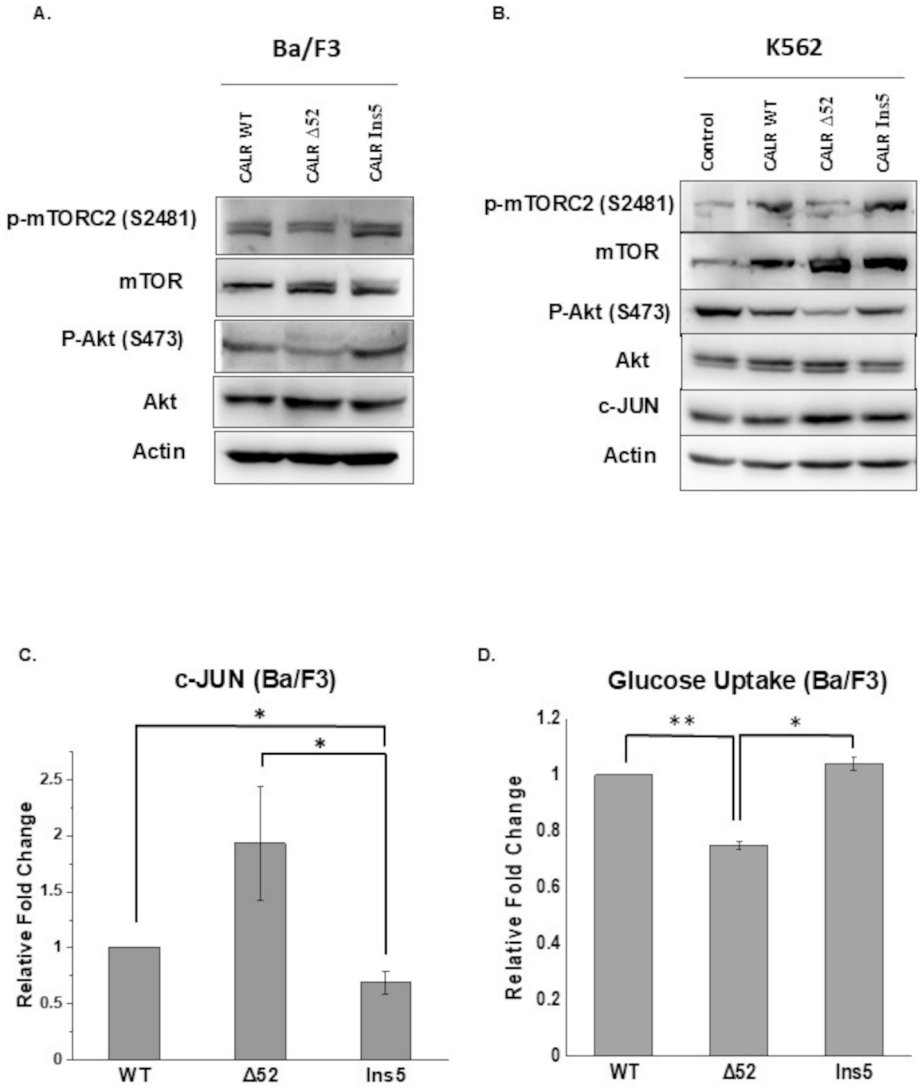

Fig. 6 c-JUN-mTORC2-AKT axis is conserved across MPN cell line models. **(A)** Representative western blots for Ba/F3 cells transduced with pMSCV-IRES-HA-mCherry-CALR-WT, CALR-Δ52, and CALR ins5 harvested for immunoblotting mTORC2 specific targets (mTOR-S2481, mTOR, Akt-S473, and Akt). Actin was used as the loading control. **(B)** Representative western blots in K562 cells electroporated with CALR-WT, CALR-Δ52, and CALR ins5 (HA-tagged CALR constructs) harvested for immunoblotting mTORC2 specific targets (mTOR-S2481, mTOR, Akt-S473, Akt and c-JUN). Actin was used as the loading control. **(C)** Real-time PCR analysis in Ba/F3 cells expressing CALR WT/Δ52/ins5 for the expression of c-JUN. Data was normalized against β-Actin. Fold change is represented as mean ± SEM. The student's t-test was used to calculate the statistical significance. **(D)** Glucose uptake in CALR WT, CALR Δ52, and CALR ins5 (mCherry tagged) expressing Ba/F3 cells were analysed by flow cytometry using 2-NBDG. CALR WT and mutants expressing cells were starved for an hour, followed by 30 min of treatment with 2-NBDG in the dark condition. Data is represented as the relative fold change with respect to CALR WT overexpressing cells. ($n = 3$). Data is represented as mean ± SEM. The statistical significance was measured through ANOVA followed by Tukey's post hoc test. Asterisk (*) indicates statistical significance. *$p < 0.05$, **$p < 0.01$

(MPN) [19, 20]. We examined the basal mTORC2 activity through its downstream effector Akt S473 in these cell lines expressing CALR WT/ CALR Δ52/ CALR ins5. CALR Δ52 expressing cells exhibited diminished mTORC2 (S2481)-specific phosphorylation and its downstream - effector phosphorylation of Akt S473 in both the cell lines (Fig. 6A and B), emphasizing our previously established result in HEK and U2OS cells (Fig. 1B and S1A). Moreover, we checked the expression of c-JUN in cells expressing CALR mutants and observed an elevated level of c-JUN in CALR Δ52 expressing cells (Fig. 6B and C). Finally, decreased basal mTORC2 activity correlated with decreased glucose uptake in Ba/F3 cells expressing CALR Δ52 (Fig. 6D). In summary, downmodulation of the mTORC2-Akt axis by c-JUN suppressed the glucose uptake, specifically in the context of Type I CALR mutations.

Discussion

Type I and II CALR mutations differed significantly in terms of patient outcome with Type I showing a better overall survival as compared to other mutations in MPN-Type II CALR mutations or JAK2V617F [7, 21]. These differences were surprising as the Type I and II mutations have been implicated in thrombopoietin receptor (TpoR) and G-CSFR signalling [6, 22, 23] without any significant difference associated with them.

Previous report indicated that a combination of mTOR or PI3K/Akt inhibitor with Ruxolitinib decreased the proliferation of myeloid progenitors [9]. This correlated with the reported deregulation of genes associated with the mTOR signalling pathway in MPN patients [24, 25]. In fact, targeting the mTOR/PI3K-Akt pathway in MPN patients with JAK2 V617F showed a therapeutic potential [26, 27]. However, these reports did not investigate the specific effects of CALR mutations. Moreover, no specific difference between Type I and II CALR mutations was reported in these experiments. It is noteworthy that the CALR mutations arising in the haematopoietic stem cell compartment were reported in both the lymphoid and myeloid lineages [10, 28]. Therefore, the mutants may exert effects independent of the TpoR or G-CSFR. Such a scenario was previously reported where Type I CALR mutations lead to abnormal cytosolic calcium [29]. CALR mutations were reported to alter the glycoproteome, an effect related to its altered chaperone function [30]. Moreover, CALR mutations were reported to upregulate oxidative stress and unfolded protein response (UPR) [19, 31, 32]. Here we report that CALR Type I mutation (CALR Δ52) suppressed basal mTORC2 signalling without affecting mTORC1. Such a downregulation was not observed in CALR ins5 mutation. Moreover, progressive truncation of CALR WT tail was sufficient to induce mTORC2 signalling. In fact, progressive truncation of the C-terminus achieved greater activation of mTORC1 and mTORC2. This indicated that CALR C-terminal tail restricted the basal activation of mTORC2. The downregulation of mTORC2- Akt S473 in the presence of CALR Δ52 prompted us to check whether PI3K/Akt-mTOR inhibitors worked differentially between Type I and II CALR mutations. To this effect, our data showed that the two mutations responded well to the PI3K/Akt-mTOR inhibitors. Therefore, a therapeutic strategy using Akt inhibition would be equally effective in CALR Type I and II mutations. Our results further showed that RICTOR was indeed downregulated by CALR Δ52. This correlated with increased expression of c-JUN in CALR Δ52 expressing cells. In fact, knockdown of c-JUN was sufficient to restore RICTOR levels and mTORC2 activity in the presence of CALR Δ52. Previous reports had shown the localization of mutant CALR proteins in different subcellular compartments, including Golgi, secretory vesicles and the nucleus [13, 33]. CALR Δ52 was reported to enhance TpoR transcription through modulation of Fli1 binding at the promoter sequences of *c-mpl* (TpoR) [14]. Our results revealed a specific enrichment of CALR Δ52 at the enhancer of *jun*. We, therefore, propose that CALR Δ52 enhances c-JUN expression through direct modulation of the chromatin. Finally, mTORC2 has been previously implicated in glucose metabolism [18]. In accordance, we observed decreased glucose uptake with CALR Δ52 along with reduced cellular ATP levels. These were reversed upon knockdown of c-JUN or overexpression of mTORC2 components RICTOR/mSIN1. Thus, we propose c-JUN-mTORC2-Akt S473 as a novel signalling target of CALR Type I mutations (Fig. 7).

Materials and methods

Cell culture and transfections

Ba/F3 CALR WT/ CALR Δ52/ CALR ins5 cell lines and K562 cell lines were cultured in RPMI media (Himedia, India) supplemented 10% FBS (Gibco, USA) and 1% penicillin and streptomycin (Himedia, India) and IL3 (speficically for Ba/F3 cell lines). HEK293 and U2OS cells are cultured in DMEM (Himedia, India) medium supplemented with 10% FBS (Gibco, USA) and 1% penicillin and streptomycin (Himedia, India) in a humidified incubator at 37 °C and 5% CO2. Transfection was performed at 70% confluency in a 60 mm adherent plate with lipofectamine 2000 (ThermoFisher) according to the manufacturer's protocol. 6ug of CALR plasmids (pcDNA 3.1-HA-CALR WT, CALR Δ52 and CALR Ins5) (The list of plasmids used in the study is mentioned in the supplementary Table 3) was used for transfection in all cases. To study the mTORC2-assembly, cells were transfected with 6ug of pcDNA 3.1-HA- CALR Δ52 (control) or co-transfected with CALR Δ52 along with Rictor, mSIN1, Rictor + mSIN1 using 6ug of plasmids and lipofectamine 2000. siRNA-mediated knockdown of c-JUN was performed using Silencer Select pre-designed and validated siRNA (Life Technologies, ThermoFisher, s7658) and Silencer Select negative control no. 1 siRNA (4390843, ThermoFisher) as the control. To knockdown the expression of c-JUN two rounds of c-JUN siRNA transfection was performed in HEK cells with the altered final concentration of 60nM in all conditions as described previously [34]. All transfected samples were harvested 24 h after the last round of transfection to be analysed by western blot, qRT-PCR or proceeded for flow cytometry as described in the respective protocols.

Immunoblotting

Cells were harvested and permeabilized in ice-cold modified RIPA buffer (0.5mM Tris HCl pH 7.5, 1 N NaCl, 0.5 M EDTA pH 8.0, 0.5 M NaF, 0.05 M Na3VO4, 10% SDS, 100mM PMSF, 10% Triton X-100, 50% glycerol)

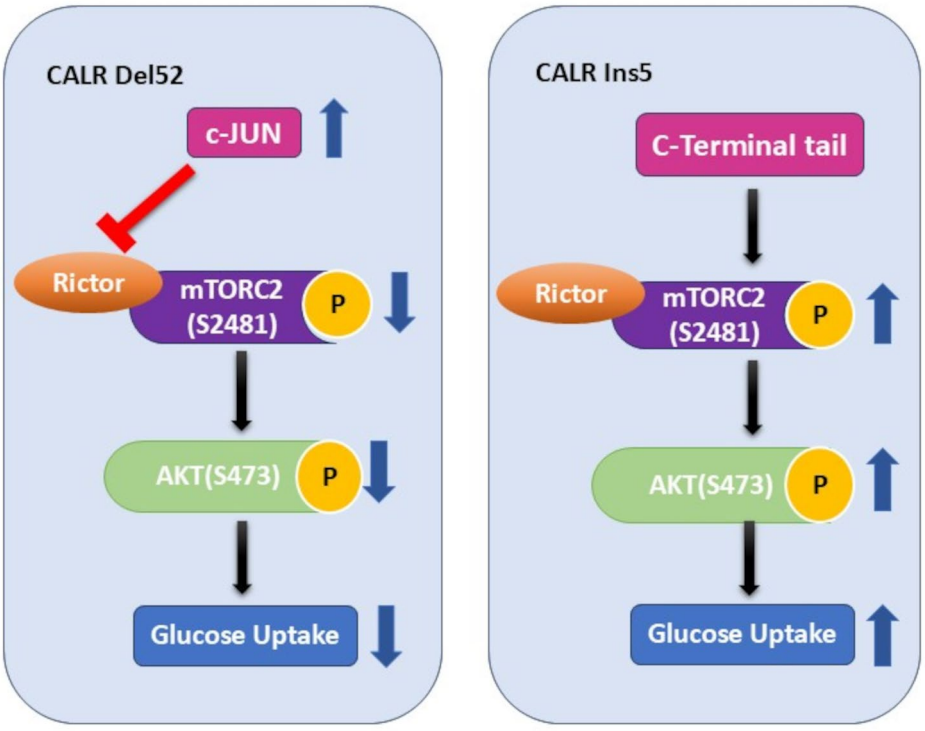

Fig. 7 Differential regulation of mTORC2 signalling by Type I and Type II calreticulin (CALR) mutations driving myeloproliferative neoplasm. Schematic diagram to delineate differential mTORC2 signalling by CALR Type I and Type II mutants. In Type I CALR mutant (CALR Δ52) expressing cells, c-JUN diminishes the mTORC2 activation through RICTOR and its downstream effector Akt S473, thereby decreasing glucose uptake in the cells. However, the C-Terminal tail of CALR is responsible for the robust mTORC2 activation, leading to increased p-Akt S473 expression level and glucose uptake in Type II CALR mutation (CALR Ins5)

with Phosphatase inhibitor (PhosSTOP from Roche # 4906845001) and centrifuged at 10,000 g for 20 min. The supernatant was collected and quantified using a BCA protein quantification assay. 50 µg protein mixed with loading dye was loaded in each lane of the SDS-PAGE gel. Proteins were transferred to a nitrocellulose membrane (BIO-RAD) followed by overnight incubation with primary antibodies (Table 1. Supplementary list of antibodies). Secondary incubation was done at room temperature for 2 h. Development of blots was done by Supersignal west femto and pico chemiluminescent substrate (ThermoFisher Scientific). Using a chemiluminescent marker, blots were imaged in a LAS 500 imager. Details of the antibodies are provided in the supplementary methods. Densitometric analysis was performed using ImageJ and normalized against Actin. (Supplementary figures).

Glucose uptake assay

Cells were incubated in serum free starvation media for an hour followed by addition of 2-NBDG (2-[N-(7-nitrobenz-2-oxa-1,3-diazol-4-yl) amino]-2-deoxy-D-glucose) for 30 min in dark. Fluorescence was detected by the FIT-C channel in the mCherry-positive population to detect the transfected population. FITC-A median was taken for each condition for the comparison.

ATP measurement assay

Cells were cultured and transfected in 96 well plate and ATP measurement assay was performed on cells 24 h post transfection as per the manufacturer's instructions (CellTitre-gloR2 Promega, #G9241). Normalisation was done for luminescence per µg of protein.

ChIP-qPCR

Cells were fixed in 1% formaldehyde, followed by sonication for shearing of DNA (200–700 bp) extracted from HEK cells expressing HA-tagged CALR WT/Δ52/ins5. 30ug of chromatin was used for incubation with anti-HA antibody for 1 h at 4˚C followed by overnight incubation with Protein A/G beads (ThermoFisher). The DNA enrichment was quantified through qPCR against IgG control sample for c-JUN promoter and distal enhancer regions. For the list of primers, please refer to the supplementary methods (Table 2).

Statistical analysis

Statistical analysis was performed using the student's t-test between two groups or ANOVA followed by Tukey's post hoc test for multiple comparisons. Graphs were plotted on Origin 2020b and GraphPad Prism.

Significance is denoted with asterisks (i.e., $*p < 0.05$, $**p < 0.01$, $***p < 0.001$).

Supplementary Information

The online version contains supplementary material available at https://doi.org/10.1186/s12964-025-02212-0.

Supplementary Material 1

Supplementary Material 2

Supplementary Material 3

Acknowledgements
We acknowledge David Pearce (UCSF, USA) and Richard Cerione (Cornell, USA) for pRK5-FLAG-RICTOR and pcDNA3.1-V5-c-JUN plasmids, respectively. We are thankful to Stefan N. Constantinescu for providing Ba/F3 CALR WT/CALR Δ52 and CALR ins5 cell lines. We thank Manoj Menon (p-Erk1/2 and Erk2 antibodies) and Sagar Sengupta (c-JUN antibody). SN, AS, SS, RKS and SC acknowledge their respective fellowships from UGC, DBT, IIT Delhi, IIT Delhi and DBT. AR acknowledges funding from DBT/Wellcome Trust India Alliance (IA/I/19/1/504285).

Author contributions
SN and AR conceptualised the project and wrote the original draft. SN standardised and performed the experiments. SN, AS and SC performed cloning and WT-truncation tail study. SS operated flow cytometry. RKS standardised the methodology for ChIP. All authors reviewed and edited the manuscript. CSD provided essential reagents and research inputs. AR supervised the project.

Data availability
No datasets were generated or analysed during the current study.

Declarations

Competing interests
The authors declare no competing interests.

Author details
[1]Kusuma School of Biological Sciences, Indian Institute of Technology Delhi, Hauz Khas, New Delhi 110016, India

Received: 24 September 2024 / Accepted: 22 April 2025
Published online: 12 May 2025

References

1. Peterson JR, Ora A, Van PN, Helenius A. Transient, lectin-like association of calreticulin with folding intermediates of cellular and viral glycoproteins. Mol Biol Cell. 1995;6:1173–84.
2. Raghavan M, Wijeyesakere SJ, Peters LR, Del Cid N. Calreticulin in the immune system: Ins and outs. Trends Immunol. 2013;34:13–21.
3. Klampfl T, Gisslinger H, Harutyunyan AS, Nivarthi H, Rumi E, Milosevic JD, et al. Somatic mutations of calreticulin in myeloproliferative neoplasms. N Engl J Med. 2013;369:2379–90.
4. Nangalia J, Massie CE, Baxter EJ, Nice FL, Gundem G, Wedge DC, et al. Somatic CALR mutations in myeloproliferative neoplasms with nonmutated JAK2. N Engl J Med. 2013;369:2391–405.
5. Marty C, Pecquet C, Nivarthi H, El-Khoury M, Chachoua I, Tulliez M, et al. Calreticulin mutants in mice induce an MPL-dependent thrombocytosis with frequent progression to myelofibrosis. Blood. 2016;127:1317–24.
6. Araki M, Yang Y, Masubuchi N, Hironaka Y, Takei H, Morishita S, et al. Activation of the thrombopoietin receptor by mutant calreticulin in CALR-mutant myeloproliferative neoplasms. Blood. 2016;127:1307–16.
7. Tefferi A, Vannucchi AM. CALR mutations possess unique prognostic relevance in myelofibrosis—before and after transplant. Bone Marrow Transpl. 2024;59:1–3.
8. Kaur A, Venkatesan A, Kandarpa M, Talpaz M, Raghavan M. Lysosomal degradation pathways target mutant calreticulin and the thrombopoietin receptor in myeloproliferative neoplasms. 2023;: 2023.07.12.548605.
9. Bartalucci N, Tozzi L, Bogani C, Martinelli S, Rotunno G, Villeval J-L, et al. Co-targeting the PI3K/mTOR and JAK2 signalling pathways produces synergistic activity against myeloproliferative neoplasms. J Cell Mol Med. 2013;17:1385–96.
10. Kjaer L, Holmström MO, Cordua S, Andersen MH, Svane IM, Thomassen M, et al. Sorted peripheral blood cells identify CALR mutations in B- and T-lymphocytes. Leuk Lymphoma. 2018;59:973–7.
11. Saxton RA, Sabatini DM. mTOR signaling in growth, metabolism, and disease. Cell. 2017;168:960–76.
12. Walker NM, Mazzoni SM, Vittal R, Fingar DC, Lama VN. c-Jun N-terminal kinase (JNK)–mediated induction of mSin1 expression and mTORC2 activation in mesenchymal cells during fibrosis. J Biol Chem. 2018;293:17229–39.
13. Pecquet C, Papadopoulos N, Balligand T, Chachoua I, Tisserand A, Vertenoeil G, et al. Secreted mutant calreticulins as rogue cytokines in myeloproliferative neoplasms. Blood. 2023;141:917–29.
14. Pronier E, Cifani P, Merlinsky TR, Berman KB, Somasundara AVH, Rampal RK, et al. Targeting the CALR interactome in myeloproliferative neoplasms. JCI Insight. 2018;3:e122703.
15. Yang G, Murashige DS, Humphrey SJ, James DE. A positive feedback loop between Akt and mTORC2 via SIN1 phosphorylation. Cell Rep. 2015;12:937–43.
16. Yan Y, An J, Yang Y, Wu D, Bai Y, Cao W, et al. Dual Inhibition of AKT-mTOR and AR signaling by targeting HDAC3 in PTEN- or SPOP-mutated prostate cancer. EMBO Mol Med. 2018;10:e8478.
17. Lin J, Sampath D, Nannini MA, Lee BB, Degtyarev M, Oeh J, et al. Targeting activated Akt with GDC-0068, a novel selective Akt inhibitor that is efficacious in multiple tumor models. Clin Cancer Res. 2013;19:1760–72.
18. Mao Z, Zhang W. Role of mTOR in glucose and lipid metabolism. Int J Mol Sci. 2018;19:2043.
19. Salati S, Genovese E, Carretta C, Zini R, Bartalucci N, Prudente Z, et al. Calreticulin Ins5 and Del52 mutations impair unfolded protein and oxidative stress responses in K562 cells expressing CALR mutants. Sci Rep. 2019;9:10558.
20. Pecquet C, Chachoua I, Roy A, Balligand T, Vertenoeil G, Leroy E, et al. Calreticulin mutants as oncogenic rogue chaperones for tpor and traffic-defective pathogenic tpor mutants. Blood. 2019;133:2669–81.
21. Guglielmelli P, Rotunno G, Fanelli T, Pacilli A, Brogi G, Calabresi L, et al. Validation of the differential prognostic impact of type 1/type 1-like versus type 2/type 2-like CALR mutations in myelofibrosis. Blood Cancer J. 2015;5:e360.
22. Chachoua I, Pecquet C, El-Khoury M, Nivarthi H, Albu R-I, Marty C, et al. Thrombopoietin receptor activation by myeloproliferative neoplasm associated calreticulin mutants. Blood. 2016;127:1325–35.
23. Elf S, Abdelfattah NS, Chen E, Perales-Patón J, Rosen EA, Ko A, et al. Mutant calreticulin requires both its mutant C-terminus and the thrombopoietin receptor for oncogenic transformation. Cancer Discov. 2016;6:368–81.
24. Čokić VP, Mossuz P, Han J, Socoro N, Beleslin-Čokić BB, Mitrović O, et al. Microarray and proteomic analyses of myeloproliferative neoplasms with a highlight on the mTOR signaling pathway. PLoS ONE. 2015;10:e0135463.
25. Kelliher S, Gamba S, Weiss L, Shen Z, Marchetti M, Schieppati F, et al. Platelet proteomic profiling reveals potential mediators of immunothrombosis and proteostasis in myeloproliferative neoplasms. Blood Adv. 2024;8:4276–80.
26. Bogani C, Bartalucci N, Martinelli S, Tozzi L, Guglielmelli P, Bosi A, et al. mTOR inhibitors alone and in combination with JAK2 inhibitors effectively inhibit cells of myeloproliferative neoplasms. PLoS ONE. 2013;8:e54826.
27. Bartalucci N, Guglielmelli P, Vannucchi AM. Rationale for targeting the PI3K/Akt/mTOR pathway in myeloproliferative neoplasms. Clin Lymphoma Myeloma Leuk. 2013;13:S307–9.
28. Olschok K, Han L, de Toledo MAS, Böhnke J, Graßhoff M, Costa IG, et al. CALR frameshift mutations in MPN patient-derived iPSCs accelerate maturation of megakaryocytes. Stem Cell Rep. 2021;16:2768–83.
29. Pietra D, Rumi E, Ferretti VV, Di Buduo CA, Milanesi C, Cavalloni C, et al. Differential clinical effects of different mutation subtypes in CALR-mutant myeloproliferative neoplasms. Leukemia. 2016;30:431–8.
30. Schürch PM, Malinovska L, Hleihil M, Losa M, Hofstetter MC, Wildschut MHE, et al. Calreticulin mutations affect its chaperone function and perturb the glycoproteome. Cell Rep. 2022;41:111689.
31. Nam AS, Kim K-T, Chaligne R, Izzo F, Ang C, Taylor J, et al. Somatic mutations and cell identity linked by genotyping of transcriptomes. Nature. 2019;571:355–60.

32. Jutzi JS, Marneth AE, Jiménez-Santos MJ, Hem J, Guerra-Moreno A, Rolles B, et al. CALR-mutated cells are vulnerable to combined Inhibition of the proteasome and the Endoplasmic reticulum stress response. Leukemia. 2023;37:359–69.
33. Liu P, Zhao L, Loos F, Marty C, Xie W, Martins I, et al. Immunosuppression by mutated calreticulin released from malignant cells. Mol Cell. 2020;77:748–e7609.
34. Lukey MJ, Greene KS, Erickson JW, Wilson KF, Cerione RA. The oncogenic transcription factor c-Jun regulates glutaminase expression and sensitizes cells to glutaminase-targeted therapy. Nat Commun. 2016;7:11321.

Publisher's note